VETOR

Complex Eigenvalues Analysis of the S_N equations for deterministic coarse-mesh methods development applied in one-dimensional neutron shielding calculations

Análise de autovalores complexos das equações S_N para desenvolvimento de métodos de malha grossa aplicados a cálculos unidimensionais de blindagem de nêutrons

Rafael Barbosa Libotte[1,†], Hermes Alves Filho[1], Fernando Carvalho da Silva[2]

[1]*Instituto Politécnico, Universidade do Estado do Rio de Janeiro, Nova Friburgo, Brasil*
[2]*COPPE, Universidade Federal do Rio de Janeiro, Rio de Janeiro, Brasil*
[†]**Corresponding author:** rafaellibotte@hotmail.com

Abstract

When using spectral nodal methods in the solution of fixed-source problems, one of the steps involves obtaining the intranodal homogeneous solution of the neutron transport equations in the discrete ordinates formulation (S_N), where an eigenvalue problem is solved. Up until now, this process involved the emergence of N (even order for Gauss-Legendre quadrature) real and symmetric eigenvalues. However, in some cases, complex conjugates may appear in this step. Thus, we present a significant innovation in this type of computational modelling, by using the Euler's Formula to manipulate the local analytical solution and achieve a possible application of coarse-mesh methods in these cases. In order to showcase this technique, we use the spectral deterministic method to solve a model-problem with different sets of Gaussian quadrature, which came to compute hundreds of complex eigenvalues in its analytical solution, where a good precision was achieved when comparing the obtained numerical results with the reference.

Keywords

Spectral analysis • Complex eigenvalues • Neutron shielding • Spectral-nodal methods • Neutron transport theory

Resumo

Quando usados métodos espectro-nodais na solução de problemas de fonte-fixa, um dos passos envolve a obtenção da solução homogênea da equação de transporte de nêutrons na formulação de ordenadas discretas (S_N), onde um problema de autovalor é resolvido. Até agora, este processo envolveu o surgimento de N (ordem par da quadratura de Gauss-Legendre) autovalores reais e simétricos. Porém, em alguns casos, complexos conjugados podem aparecer neste passo. Portanto, apresentamos uma significante inovação neste tipo de modelagem computacional, usando a fórmula de Euler para manipular a solução analítica local para possibilitar a aplicação de métodos de malha grossa nestes casos. A fim de mostrar esta técnica, usamos o *spectral deterministic method* para resolver um problema-modelo com diferentes ordens de quadratura Gaussiana, onde foram computados centenas de autovalores complexos na solução analítica, e um resultado com boa precisão foi atingido quando comparado com o método numérico de referência.

Palavras-chave

Análise espectral • Autovalores complexos • Blindagem de nêutrons • Métodos espectro-nodais • Teoria de transporte de nêutrons

1 Introduction

Simulating realistic neutron transport problems is essential in numerous fields of study, such as electricity generation and oil prospecting. Since the neutron transport equation has an analytical solution only for very simplified cases, many researchers work on the development of numerical methods that are capable of solving more complex fixed-source problems.

The numerical methods can be categorized into two groups: fine-mesh and coarse-mesh methods. In one-dimensional slab geometry, the fine-mesh methods can use linear approximations for the neutron angular flux, in a spatial subdomain (mesh) where the physical-material parameters are uniform, with the Diamond Difference (DD) [1] method standing as a reference even to this day. On the other hand, coarse-mesh methods, such as the Spectral Deterministic Method (SDM) [2], Modified Spectral Deterministic (MSD) [3], spectral Green's function (SGF) [4], Response Matrix (RM) [5] and Analytical Discrete Ordinates (ADO) [6], uses a set of intranodal analytical solutions, where eigenvalue problems and linear systems of equations must be solved to compute a local solution with homogeneous and particular components.

As already seen in eigenvalue problems using spectral-nodal methods [7, 8, 9], the solution of this problem can compute complex eigenvalues and eigenvectors. However, in one-dimensional neutron shielding (fixed-source) problems, with the use of the deterministic model of the neutron transport equation, in the formulation of discrete ordinates, these characteristics of the eigenvalues and respective eigenvectors, had not yet been reported. In this paper, we present a multigroup one-dimensional fixed-source problem which led to complex eigenvalues and eigenvectors. Since the neutron angular flux is a real function, these eigenvalues and eigenvectors are treated in order to enable numerical methods to be directly applied. For this, we use the Euler's formula and a rearrangement of the intranodal analytical solution that leads to an equation which contains only real variables.

Now, let us demonstrate the composition of this paper. In Section 2, we show the application of the S_N multigroup neutron transport equation in one-dimensional stationary fixed-source problems, along with presenting its local solution. Moving on to Section 3, we provide a comprehensive treatment of complex eigenvalues and eigenvectors and the manipulations involved in this system of equations. In Section 4, we showcase the numerical solution of a model problem with complex eigenvalues and eigenvectors and compare it to a fine-mesh reference (DD method) for accuracy. Finally, in Section 5, we draw insightful conclusions based on the tests conducted throughout this study.

2 Neutron Transport Equation

The intranodal stationary one-dimensional multigroup neutron transport S_N equation is written in the form [1]:

$$\mu_m \frac{\mathrm{d}}{\mathrm{d}x}\psi_{m,g}(x) + \sigma_{T,g,j}\psi_{m,g}(x) = \frac{1}{2}\sum_{g'=1}^{G}\left[\sum_{l=0}^{L}(2l+1)\sigma_{Sl,j}^{g'\to g}P_l(\mu_m)\sum_{n=1}^{N}P_l(\mu_n)\psi_{n,g}(x)\omega_n\right] + Q_{g,j},\ m = 1:N, g = 1:G. \quad (1)$$

where $\psi_{m,g}(x)$ represents the neutron angular flux in position x of energy group g travelling in the discrete direction m, μ_m and ω_m are respectively the discrete ordinates, consisting of the roots and the weights of Legendre polynomials of order N, $\sigma_{T,g,j}$ is the total macroscopic cross section and $\sigma_{Sl,j}^{g'\to g}$ is the l'th order macroscopic scattering cross sections from group g' to g in region j. The terms $P_l(\mu_n)$ are the l'th degree Legendre Polynomials, and $Q_{g,j}$ is an external fixed-source of neutrons.

The intranodal neutron transport equation has a general local analytical solution, that can be written as a sum of a homogeneous component ($\psi_{m,g}^h(x)$) and a particular one $\psi_{m,g}^p$ [4], in the form:

$$\psi_{m,g}(x) = \psi_{m,g}^h(x) + \psi_{m,g}^p,\ m = 1:N, g = 1:G. \quad (2)$$

As the particular solution has the same behavior as the external source of neutrons, this component will also be a constant. Substituting $\psi_{m,g}^p$ in Eq.(1), leads to a system of linear equations in the form:

$$\sum_{g'=1}^{G}\sum_{n=1}^{N}\left(\sigma_{T,g,j}\delta_{m,n}\delta_{g',g} - \frac{1}{2}\sum_{l=0}^{L}(2l+1)P_l(\mu_m)\sigma_{Sl,j}^{g'\to g}P_l(\mu_n)\omega_n\right)\psi_{m,g}^p = Q_{g,j},\ j = 1:J, m = 1:N, g = 1:G. \quad (3)$$

This system of equations has an analytical solution, by inverting the system of equations in the left hand-side and multiplying it to the vector composed by the equations in the right hand-side of the system. This computes a set of NG particular solutions for each discretized spatial node Γ_j [4]. For the homogeneous component of the solution, we assume this component has an exponential behavior, then when the variable $\psi^h_{m,g}(x)$ is substituted in Eq.(1), it leads to an eigenvalue problem in the form:

$$\sum_{g'=1}^{G}\sum_{n=1}^{N}\left[\frac{\delta_{mn}\delta_{g'g}\sigma_{T,g,j}}{\mu_m}-\frac{\omega_n}{2\mu_m}\sum_{l=0}^{N-1}(2l+1)\sigma_{Sl,j}^{g'\to g}P_l(\mu_m)P_l(\mu_n)\right]A_{n,g'}(\lambda)=\lambda A_{m,g}(\lambda),\ m=1:N, g=1:G. \quad (4)$$

The solution of this problem generates a set of NG eigenvalues and its correspondent eigenvectors.

In possession of the homogeneous and particular components, the general intranodal solution of the S_N neutron transport equation EQ1 can be rewritten as

$$\psi_{m,g}(x)=\sum_{l=1}^{NG}\alpha_l A_{m,g}(\lambda_l)e^{-\lambda_l(x-x_j)}+\psi^p_{m,g}, \quad (5)$$

where α_l are coefficients to be determined in each discretized spatial node using local boundary conditions. Imposing continuity conditions among the node's interfaces, this solution can be extended to all regions of the simulated model."

3 Complex Eigenvalues Treatment

The solution of the eigenvalue problem in Eq. (4) leads to a set of NG eigenvalues, and its correspondents eigenvectors, which, in some cases, might have complex components of small magnitude, when compared to its correspondents real part

The solution of the eigenvalues problem in Eq. (4), which is constituted by a non-symmetric associated matrix, leads to a set of NG eigenvalues, and its correspondents eigenvector, which, in some cases, might have complex components, depending on the physical material parameters. Although having a small magnitude, when compared to its correspondents real part (reaching as low as 10^{-9} ratio, as will be seen in the numerical results section), it is enough to avoid numerical methods to work properly, if these are not properly handled. The eigenvalue problem was solved with the Alglib linear algebra library, using the QR decomposition function for unsymmetrical matrices [10].

Now, considering a case with L real eigenvalues, and $2NC$ complete complex eigenvalues, with a ϑ_l real part and a θ_l complex part, let us organize these as shown in Figure 1.

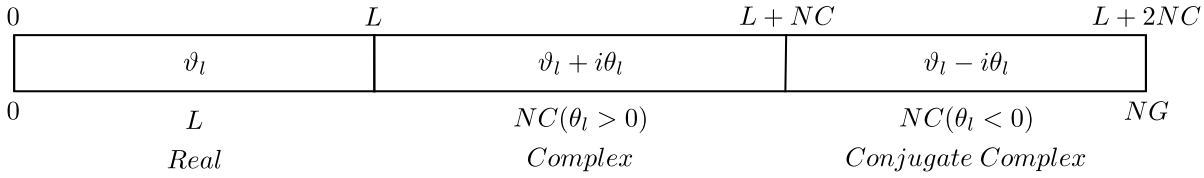

Figure 1: Eigenvalues organization

In fixed source problems, the eigenvalues and its correspondent eigenvectors are calculated, from the matrix, once, in each region where the physical parameters of the material are different and uniform and used throughout the entire iterative process. As these variables treatment are heavily dependant on matrices operations, it is important to adopt an organization for the eigenvalues and its correspondent eigenvectors.

Let us make definitions for the real eigenvalues and eigenvectors as

$$\lambda_l \equiv \vartheta_l \quad (6)$$

$$A_{g,m}(\lambda_l) \equiv a_{g,m,l}, l=1:L, \quad (7)$$

and for the complex ones as

$$\lambda_l \equiv \vartheta_l + i\theta_l \tag{8}$$
$$A_{g,m}(\lambda_l) \equiv a_{g,m,l} + ib_{g,m,l}, l = L+1 : L+NC \tag{9}$$

and

$$\lambda_l \equiv \vartheta_l - i\theta_l \tag{10}$$
$$A_{g,m}(\lambda_l) \equiv a_{g,m,l} - ib_{g,m,l}, l = L+NC+1 : L+2NC. \tag{11}$$

Using the definitions of Eqs. (7)-(11), the homogeneous part of the solution can be written as a set of 3 sums, one for the real eigenvalues, one for the complex ones and one to the conjugate complex. With this notation, it can be written:

$$\psi_{g,m}(x) = \sum_{l=1}^{L} \alpha_l a_{g,m,l} e^{\left(-\vartheta_l (x-x_j)\right)} + \sum_{l=L+1}^{L+NC} \alpha_l (a_{g,m,l} + ib_{g,m,l})) e^{\left(-(\vartheta_l + i\theta_l))(x-x_j)\right)} + \sum_{l=L+1}^{L+NC} \alpha_{l+NC} (a_{g,m,l} - ib_{g,m,l})) e^{\left(-(\vartheta_l - i\theta_l))(x-x_j)\right)} + \psi^p_{m,g}. \tag{12}$$

In order to treat the complex variables in Eq. (12), let us consider the Euler's Formula, given by

$$e^{iY} = \cos(Y) + i\sin(Y). \tag{13}$$

Substituting this formula in the Eq. (12), we can rewrite the intranodal analytical solution without any complex component in exponentials, in the form:

$$\psi_{g,m}(x) = \sum_{l=1}^{L} \alpha_l a_{g,m,l} e^{\left(-\vartheta_l (x-x_j)\right)} + \sum_{l=L+1}^{L+NC} e^{\left(-\vartheta (x-x_j)\right)} \{(\alpha_l + \alpha_{l+NC}) \left[a_{g,m,l} \cos(\theta_l (x-x_j)) + b_{g,m,l} \sin(\theta_l (x-x_j))\right] + i(\alpha_l - \alpha_{l+NC}) \left[b_{g,m,l} \cos(\theta_l (x-x_j)) - a_{g,m,l} \sin(\theta_l (x-x_j))\right]\} + \psi^p_{m,g}. \tag{14}$$

Since $\psi_{g,m}(x)$ is a real function, the coefficients α_l must be a conjugate complex of α_{l+NC}. Thus, we assume $\alpha_l = \beta_l - i\gamma_l$ and $\alpha_{l+NC} = \beta + i\gamma_l$. At this point, we must find a way to eliminate the complex numbers i. For this, we sum and subtract the definitions in order to manipulate Eq.(14). In this step, we have:

$$\alpha_l + \alpha_{l+NC} = 2\beta_l \tag{15}$$

and

$$\alpha_l - \alpha_{l+NC} = -2i\gamma_l. \tag{16}$$

Using Eqs. (15) and (16) and reorganizing Eq. (14), leads us to

$$\psi_{g,m}(x) = \sum_{l=1}^{L_1} \alpha_l a_{g,m,l} e^{-|\vartheta_l|(x-x_j)} + \sum_{l=L_1+1}^{L} \alpha_l a_{g,m,l} e^{|\vartheta_l|(x-x_j)} + \sum_{l=L+1}^{L+M} 2\beta_l e^{-|\vartheta_l|(x-x_j)} \{a_{g,m,l} \cos(\theta_l (x-x_j)) + b_{g,m,l} \sin(\theta_l (x-x_j))\} + \sum_{l=L+M+1}^{L+NC} 2\beta_l e^{|\vartheta_l|(x-x_j)} \{a_{g,m,l} \cos(\theta_l (x-x_j)) + b_{g,m,l} \sin(\theta_l (x-x_j))\} + \sum_{l=L+1}^{L+M} 2\gamma_l e^{-|\vartheta_l|(x-x_j)} \{b_{g,m,l} \cos(\theta_l (x-x_j)) - b_{g,m,l} \sin(\theta_l (x-x_j))\} + \sum_{l=L+M+1}^{L+NC} 2\gamma_l e^{-|\vartheta_l|(x-x_j)} \{b_{g,m,l} \cos(\theta_l (x-x_j)) - b_{g,m,l} \sin(\theta_l (x-x_j))\} + \psi^p_{m,g}, \tag{17}$$

where L_1 represents the number of positive real eigenvalues, and M represents the number of complex eigenvalues with positive real component. In this notation, all the eigenvalues complex components (θ_l) are positive.

Now, we can use the Eq. (17) to the left ($x = x_{j-1/2}$) and right ($x = x_{j+1/2}$) nodal interfaces. But since the exponential present in Eq. (17) may cause overflow problems, let us multiply and divide the terms inside the sums by $e^{(-|\vartheta_l|h_j/2)}$. After this step, for the right interface of the Γ_j node, we have

$$\begin{aligned}\psi_{g,m}(x_{j+1/2}) = &\sum_{l=1}^{L_1} \widehat{\alpha}_l a_{g,m,l} e^{-|\vartheta_l|h_j} + \sum_{l=L_1+1}^{L} \widehat{\alpha}_l a_{g,m,l} + \\ &+ \sum_{l=L+1}^{L+M} \widehat{\alpha}_l e^{-|\vartheta_l|h_j} \left\{a_{g,m,l}\cos(\theta_l h_j/2) + b_{g,m,l}\sin(\theta_l h_j/2)\right\} + \\ &+ \sum_{l=L+M+1}^{L+NC} \widehat{\alpha}_l \left\{a_{g,m,l}\cos(\theta_l h_j/2) + b_{g,m,l}\sin(\theta_l h_j/2)\right\} + \\ &+ \sum_{l=L+1}^{L+M} \widehat{\alpha}_{l+NC} e^{-|\vartheta_l|h_j} \left\{b_{g,m,l}\cos(\theta_l h_j/2) - a_{g,m,l}\sin(\theta_l h_j/2)\right\} + \\ &+ \sum_{l=L+M+1}^{L+NC} \widehat{\alpha}_{l+NC} \left\{b_{g,m,l}\cos(\theta_l h_j/2) - a_{g,m,l}\sin(\theta_l h_j/2)\right\} + \psi^p_{m,g}, \quad (18)\end{aligned}$$

and for the left interface

$$\begin{aligned}\psi_{g,m}(x_{j-1/2}) = &\sum_{l=1}^{L_1} \widehat{\alpha}_l a_{g,m,l} + \sum_{l=L_1+1}^{L} \widehat{\alpha}_l a_{g,m,l} e^{-|\vartheta_l|h_j} + \\ &+ \sum_{l=L+1}^{L+M} \widehat{\alpha}_l \left\{a_{g,m,l}\cos(\theta_l h_j/2) - b_{g,m,l}\sin(\theta_l h_j/2)\right\} + \\ &+ \sum_{l=L+M+1}^{L+NC} \widehat{\alpha}_l e^{-|\vartheta_l|h_j} \left\{a_{g,m,l}\cos(\theta_l h_j/2) - b_{g,m,l}\sin(\theta_l h_j/2)\right\} + \\ &+ \sum_{l=L+1}^{L+M} \widehat{\alpha}_{l+NC} e^{-|\vartheta_l|h_j} \left\{b_{g,m,l}\cos(\theta_l h_j/2) + a_{g,m,l}\sin(\theta_l h_j/2)\right\} + \\ &+ \sum_{l=L+M+1}^{L+NC} \widehat{\alpha}_{l+NC} e^{-|\vartheta_l|h_j} \left\{b_{g,m,l}\cos(\theta_l h_j/2) + a_{g,m,l}\sin(\theta_l h_j/2)\right\} + \psi^p_{m,g}. \quad (19)\end{aligned}$$

where $\widehat{\alpha}_l$ can be defined as

$$\widehat{\alpha}_l \equiv \begin{cases} \dfrac{\alpha_l}{e^{(-|\vartheta_l|h_j/2)}}, \text{ for } l = 1 : L \\ \dfrac{2\beta_l}{e^{(-|\vartheta_l|h_j/2)}}, \text{ for } l = L+1 : L+NC \\ \dfrac{2\gamma_l}{e^{(-|\vartheta_l|h_j/2)}}, \text{ for } l = L+NC+1 : L+2NC. \end{cases}$$

4 Numerical Results

In this section, a one-dimensional problem, that presents complex eigenvalues and eigenvectors is solved. The coarse-mesh method used is the Spectral Deterministic Method (SDM) [2]. The numerical results for the neutron scalar fluxes are compared with a fine-mesh reference, using the Diamond Difference method.

In this model-problem, we study a 4 group heterogeneous case, with 4 different physical-material zones [3]. The geometry of this problem can be seen in Figure 2. The left boundary condition has prescribed angular scalar fluxes $\psi_{m,g,1/2} = 1.00\ cm^{-2}s^{-1}sr$, and vacuum in the right boundary, with no external neutron sources. The total macroscopic cross-section is $\sigma_{T,g,j} = 1.0\ cm^{-1}$ for all energy groups and regions, and the macroscopic scattering cross-section of each material zone are shown in Tables 1-4.

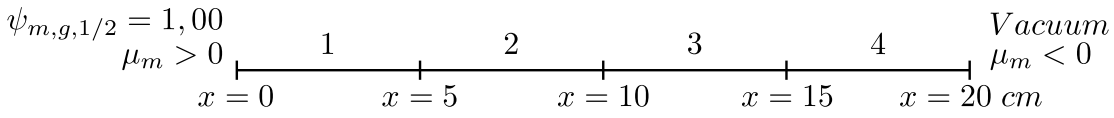

Figure 2: Model-problem 1 geometry and material zones configuration

Table 1: Material zone 1

Group	$\sigma_{S0}^{1\to g}$	$\sigma_{S0}^{2\to g}$	$\sigma_{S0}^{3\to g}$	$\sigma_{S0}^{4\to g}$
$g = 1$	0.55	0.00	0.00	0.00
$g = 2$	0.22	0.60	0.00	0.00
$g = 3$	0.10	0.20	0.45	0.00
$g = 4$	0.05	0.10	0.25	0.55

Table 2: Material zone 2

Group	$\sigma_{S0}^{1\to g}$	$\sigma_{S0}^{2\to g}$	$\sigma_{S0}^{3\to g}$	$\sigma_{S0}^{4\to g}$
$g = 1$	0.60	0.00	0.00	0.00
$g = 2$	0.15	0.65	0.00	0.00
$g = 3$	0.09	0.15	0.70	0.00
$g = 4$	0.05	0.07	0.20	0.50

The neutron scalar fluxes were calculated in each region's interface. The stopping criterion is calculated using the neutron scalar fluxes between two subsequent iterations as:

$$\left(\frac{\phi_{g,j-1/2}^{(k)} - \phi_{g,j-1/2}^{(k-1)}}{\phi_{g,j-1/2}^{(k-1)}} \right) \times 100\% < \xi,\ j = 1 : J+1, \tag{20}$$

where ξ represents a pre-estabilished tolerance, $\xi = 10^{-6}$ in all problems executed here, k represents the iteration number, and the neutron scalar flux is calculated as:

$$\phi_{g,j-1/2} = \sum_{n=1}^{N} \omega_n \psi_{n,g}(x_{j-1/2}),\ g = 1 : G, j = 1 : J-1. \tag{21}$$

This model is solved using 3 Gaussian quadrature orders, $N = 4$, 16 and a more computationally expensive one with $N = 256$, which led to the computing of hundreds of complex eigenfunctions. A reference numerical result was calculated using the the diammond difference method, with 5000 nodes in each region. The reference mesh was refined until the neutron scalar fluxes did not change within the sixth decimal place. Since the MSD method is free of truncation error, it was used only 1 node per region.

4.1 Gaussian-Legendre Quadrature $N = 4$

The solution of this model-problem with a Gaussian quadrature of order 4, leads to a set of 16 eigenvalues (being 4 energy groups × 4 discrete directions) for each material-zone. In this case, 4 complex eigenvalues were computed in material zones 1 and 4 each. Table 5 shows these eigenvalues with the positive complex parts, although the conjugates were also computed.

Table 5: Complex eigenvalues in model-problem 1 - S_4.

Material zone	ϑ	θ
1	9.579302e-01	2.233328e-08
	-9.579302e-01	5.683020e-09
4	2.341383e+00	5.100480e-08
	9.226372e-01	2.895429e-08

The numerical results for the neutrons scalar fluxes using Gaussian quadrature $N = 4$ are shown in Table 6, with the relative percentage deviation between the MSD and the reference inside the parenthesis.

Table 3: Material zone 3

Group	$\sigma_{S0}^{1\to g}$	$\sigma_{S0}^{2\to g}$	$\sigma_{S0}^{3\to g}$	$\sigma_{S0}^{4\to g}$
$g=1$	0.65	0.00	0.00	0.00
$g=2$	0.18	0.75	0.00	0.00
$g=3$	0.08	0.12	0.68	0.00
$g=4$	0.02	0.08	0.22	0.60

Table 4: Material zone 4

Group	$\sigma_{S0}^{1\to g}$	$\sigma_{S0}^{2\to g}$	$\sigma_{S0}^{3\to g}$	$\sigma_{S0}^{4\to g}$
$g=1$	0.45	0.00	0.00	0.00
$g=2$	0.30	0.60	0.00	0.00
$g=3$	0.12	0.18	0.63	0.00
$g=4$	0.07	0.14	0.21	0.60

Table 6: Neutron scalar fluxes for $(cm^{-2}s^{-1})$ for model-problem 1 - S_4

Method	Group	$x=0\ cm$	$x=5\ cm$	$x=10\ cm$	$x=15\ cm$	$x=20\ cm$
DD	1	5.985087×10^{-1}	3.081410×10^{-3}	3.285798×10^{-5}	3.615141×10^{-7}	1.607666×10^{-9}
	2	6.188975×10^{-2}	3.865135×10^{-3}	7.631446×10^{-5}	1.904389×10^{-6}	1.428770×10^{-8}
	3	3.548206×10^{-2}	3.531797×10^{-3}	1.263835×10^{-4}	2.908361×10^{-6}	3.257054×10^{-8}
	4	2.920117×10^{-2}	4.296231×10^{-3}	1.212879×10^{-4}	4.085070×10^{-6}	5.729438×10^{-8}
MSD	1	5.985087×10^{-1} (0)	3.081417×10^{-3} (0,00022717)	3.285813×10^{-5} (0.00045651)	3.615164×10^{-7} (0.00063621)	1.607680×10^{-9} (0.00087083)
	2	6.188975×10^{-2} (0)	3.865139×10^{-3} (0.00010349)	7.631468×10^{-5} (0.00028828)	1.904397×10^{-6} (0.00042008)	1.428780×10^{-8} (0.00069990)
	3	3.548206×10^{-2} (0)	3.531801×10^{-3} (0.00011326)	1.263838×10^{-4} (0.00023737)	2.908372×10^{-6} (0.00037822)	3.257075×10^{-8} (0.00064475)
	4	2.920117×10^{-2} (0)	4.296234×10^{-3} (0.00006983)	1.212882×10^{-4} (0.00024735)	4.085085×10^{-6} (0.00036719)	5.729475×10^{-8} (0.00064579)

4.2 Gaussian-Legendre Quadrature $N = 16$

Using the $N = 16$ Gaussian quadrature set, 8 complex eigenvalues were computed for the first material zone, and 16 for the fourth one. As the S_4 case, the eigenvalues with positive complex components are shown in Table 7, but its conjugates were also computed.

Table 7: Complex eigenvalues in model-problem 1 - S_{16}.

Material zone	ϑ	θ
1	1.541449e+00	7.382977e-09
	1.026697e+00	2.275965e-10
	-2.074201e+00	1.355041e-08
	-1.110299e+00	4.085901e-09
4	9.925055e+00	4.662198e-08
	3.351517e+00	3.276860e-08
	1.534416e+00	2.951119e-09
	1.025103e+00	1.788802e-09
	-2.064213e+00	2.270793e-08
	-1.534416e+00	2.113968e-08
	-9.073326e-01	1.296608e-08
	-1.025103e+00	4.218374e-09

The results for the neutron scalar fluxes in the region's interfaces are displayed in Table 8, alongside the percentage deviations, as in the $N = 4$ case.

Table 8: Neutron scalar fluxes ($cm^{-2}s^{-1}$) for model-problem 1 - S_{16}

Method	Group	$x = 0\ cm$	$x = 5\ cm$	$x = 10\ cm$	$x = 15\ cm$	$x = 20\ cm$
DD	1	5.985087×10^{-1}	3.021477×10^{-3}	3.335254×10^{-5}	3.876153×10^{-7}	1.847463×10^{-9}
	2	6.188974×10^{-2}	3.834792×10^{-3}	7.578095×10^{-5}	1.932782×10^{-6}	1.475540×10^{-8}
	3	3.548202×10^{-2}	3.514151×10^{-3}	1.251785×10^{-4}	2.919238×10^{-6}	3.306714×10^{-8}
	4	2.920117×10^{-2}	4.268252×10^{-3}	1.201737×10^{-4}	4.094509×10^{-6}	5.778184×10^{-8}
MSD	1	5.985087×10^{-1} (0)	3.021478×10^{-3} (0.00003310)	3.335257×10^{-5} (0.00008995)	3.876157×10^{-7} (0.00010320)	1.847466×10^{-9} (0.00016238)
	2	6.188974×10^{-2} (0)	3.834793×10^{-3} (0.00002608)	7.578099×10^{-5} (0.00005278)	1.932784×10^{-6} (0.00010348)	1.475542×10^{-8} (0.00013554)
	3	3.548202×10^{-2} (0)	3.514152×10^{-3} (0.00002846)	1.251785×10^{-4} (0)	2.919240×10^{-6} (0.00006851)	3.306719×10^{-8} (0.00015121)
	4	2.919957×10^{-2} (0.00547923)	4.268194×10^{-3} (0.00135887)	1.201733×10^{-4} (0.00033285)	4.094517×10^{-6} (0.00019538)	5.778195×10^{-8} (0.00019037)

4.3 Gaussian-Legendre Quadrature $N = 256$

A more computationally expensive Gaussian quadrature set was also used in the solution of this model-problem. With $N = 256$, hundreds of eigenvalues were computed. As in this case, a large amount of eigenfunctions are obtained, these are better displayed in a chart, as shown in Figure 3, where the eigenvalues in regions 1 and 4 are respectively represented by the blue and orange dots, with real component (ϑ) in the $x-$axis and complex component in the $y-$axis (θ). As in the previous eigenvalues tables, in this figure, only the eigenvalues with positive complex components are displayed, but its conjugates are also computed.

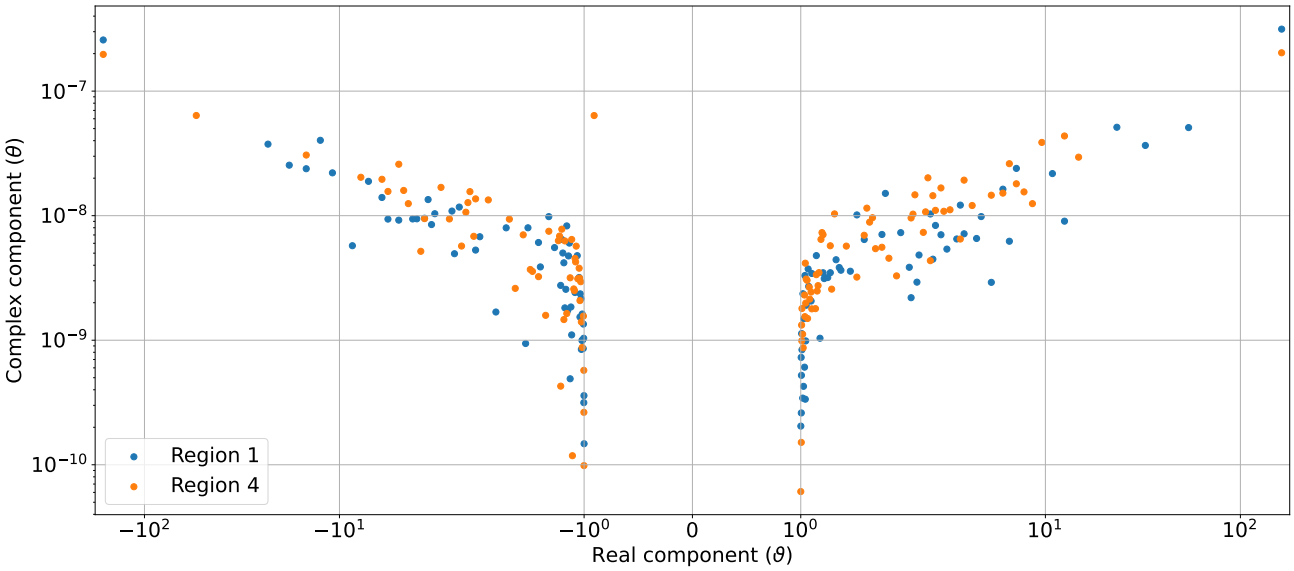

Figure 3: Complex eigenvalues representation - S_{256}

The numerical results for the neutron scalar fluxes in the $N = 256$ case are shown in Table 9, alongside the percentage deviation.

Table 9: Neutron scalar fluxes ($cm^{-2}s^{-1}$) for model-problem 1 - S_{256}

Method	Group	$x = 0\ cm$	$x = 5\ cm$	$x = 10\ cm$	$x = 15\ cm$	$x = 20\ cm$
DD	1	5.985087×10^{-1}	3.020339×10^{-3}	3.334018×10^{-5}	3.874016×10^{-7}	1.846105×10^{-9}
	2	6.188974×10^{-2}	3.832744×10^{-3}	7.574997×10^{-5}	1.931736×10^{-6}	1.474215×10^{-8}
	3	3.548202×10^{-2}	3.512730×10^{-3}	1.251151×10^{-4}	2.917859×10^{-6}	3.303602×10^{-8}
	4	2.920117×10^{-2}	4.265850×10^{-3}	1.201241×10^{-4}	4.092650×10^{-6}	5.772684×10^{-8}
MSD	1	5.985087×10^{-1} (0)	3.020340×10^{-3} (0.00003311)	3.334020×10^{-5} (0.00005999)	3.874019×10^{-7} (0.00007744)	1.846108×10^{-9} (0.00016250)
	2	6.188937×10^{-2} (0.00059783)	3.832722×10^{-3} (0.00057400)	7.574966×10^{-5} (0.00040924)	1.931731×10^{-6} (0.00025883)	1.474213×10^{-8} (0.00013567)
	3	3.548157×10^{-2} (0.00126824)	3.512698×10^{-3} (0.00091097)	1.251143×10^{-4} (0.00063941)	2.917846×10^{-6} (0.00044553)	3.303592×10^{-8} (0.00030270)
	4	2.919278×10^{-2} (0.02873172)	4.265467×10^{-3} (0.00897828)	1.201205×10^{-4} (0.00299690)	4.092595×10^{-6} (0.00134387)	5.772639×10^{-8} (0.00016238)

4.4 Results analysis

The numerical results obtained in the solution of this model-problem showed that the proposed complex eigenvalues treatment was efficient. With the $N = 4$ Gaussian quadrature order, the coarse-mesh method was able to compute neutron scalar fluxes with the same 6 decimal places as the reference in the leftmost interface of the spatial domain, with the biggest percentage deviation of 0.00087083 % in $x = 20$ cm. For the $N = 16$ case, similar behaviour was achieved, with exact 6 decimal places of precision in the neutron scalar flux in some energy groups in positions $x = 0$ and 10 cm, having the most amount of deviation being 0.00547923 %. Now, analyzing the numerical results for the most expensive case studied here, the MSD was able to reach at least 0.02873172 % of precision when compared to the reference, even reaching all 6 decimal places of precision in $x = 0$ for one of the energy groups.

5 Concluding Remarks

In this work, a technique to treat complex eigenvalues in applied in neutron shielding problems is presented. It relies on the rearrangement of the neutron transport equations local analytical solution, using the Eulers Formula, where the complex eigenfunctions, which haven't been seen in one-dimensional problems yet, are transformed in an equivalent real system of equations.

A model problem with 4 energy group was solved, using $N = 4, 16$ and 256 Gaussian quadrature orders, where in each case a set of complex conjugate eigenvalues were computed. This treatment was implemented within the Spectral Deterministic Method, which enabled its usage in cases with complex eigenvalues. The numerical results achieved with the SDM were compared with the fine-mesh reference method Diamond Difference. In all studied cases, this technique led to an intranodal analytical solution that enabled the coarse-mesh method to solve the model-problem with good accuracy, even achieving all 6 decimal places of precision in some positions when compared to the reference. When considering the $N = 256$ case, this treatment allowed the problem to be solved with the highest deviation being lesser than 0.1 %, despite having hundreds of complex eigenvalues.

Analyzing the computed complex eigenvalues in all studied cases here, we were able to conclude that even for eigenvalues with θ_l/ϑ_l ratios smaller than 10^{-10} magnitude, it would not be solved considering only the real part of these variables, which led the SDM errors during the iterative process. For future works, we intend to apply this technique to multidimensional problems, and solve problems with higher number of energy groups.

Acknowledgements

This study was financed in part by the Coordenação de Aperfeiçoamento de Pessoal de Nível Superior – Brasil (CAPES) – Finance Code 001. Rafael Libotte is supported by a doctoral fellowship from the Carlos Chagas Filho Foundation for Supporting Research in the State of Rio de Janeiro, Grant No. E-26/201.278/2023.

References

[1] E. E. Lewis and W. F. Miller, *Computational methods of neutron transport*, 2nd ed. New York: Wiley, 1993.

[2] A. M. Oliva, "Método espectral determinístico para a solução de problemas de transporte de nêutrons usando a formulação das ordenadas discretas," Ph.D. dissertation, Programa de Pós-Graduação em Modelagem Computacional, IPRJ/UERJ, Nova Friburgo, Brasil, 2018, in Portuguese. Available at: http://www.bdtd.uerj.br/handle/1/13719

[3] R. B. Libotte, "Método de malha grossa para solução numérica de problemas de blindagem de nêutrons em geometria unidimensional na formulação de ordenadas discretas com perspectivas a cálculos multidimensionais em geometria retangular," Master's thesis, Programa de Pós-Graduação em Modelagem Computacional, IPRJ/UERJ, Nova Friburgo, Brasil, 2021, in Portuguese. Available at: http://www.bdtd.uerj.br/handle/1/16461

[4] R. C. de Barros, "A spectral nodal method for the solution of discrete ordinates problems in one- and two-dimensional cartesian geometry," Ph.D. dissertation, University of Michigan, UMICH, Ann Arbor, Estados Unidos, 2018. Available at: https://deepblue.lib.umich.edu/handle/2027.42/105093

[5] O. P. da Silva, "Um método de matriz resposta para cálculos de transporte multigrupos de energia na formulação de ordenadas discretas em meios não-multiplicativos," Ph.D. dissertation, Programa de Pós-Graduação em Modelagem Computacional, IPRJ/UERJ, Nova Friburgo, Brasil, 2018, in Portuguese. Available at: http://www.bdtd.uerj.br/handle/1/13715

[6] L. B. Barichello, L. C. Cabrera, and J. F. Prolo Filho, "An analytical approach for a nodal scheme of two-dimensional neutron transport problems," *Annals in Nuclear Energy*, vol. 38, pp. 1310–1317, 2011. Available at: https://doi.org/10.1016/j.anucene.2011.02.004

[7] M. P. de Abreu, "Métodos determinísticos livres de aproximações espaciais para a solução numérica dominante de problemas de autovalor multiplicativo na formulação de ordenadas discretas da teoria do transporte de nêutrons," Ph.D. dissertation, COPPE/UFRJ, Rio de Janeiro, Brasil, 1996, in Portuguese.

[8] S. A. Ramírez, "Cálculos de criticalidade usando a equação de transporte de nêutrons multigrupo unidimensional na formulação das ordenadas discretas a partir da solução analítica local," Ph.D. dissertation, Programa de Pós-Graduação em Modelagem Computacional, IPRJ/UERJ, Nova Friburgo, Brasil, 2021, in Portuguese. Available at: http://www.bdtd.uerj.br/handle/1/16896

[9] R. B. Libotte, H. Alves Filho, and F. C. da Silva, "Technique for reducing time in the calculation ofeigenvalues and eigenvectors applied in neutrontransport fixed-source problems," *Vetor*, vol. 33, no. 1, 2023. Available at: https://doi.org/10.14295/vetor.v33i1.15155

[10] S. Bochkanov, "Alglib." Available at: www.alglib.net